Yokohama Publishers
ISSN 1349-8169 ONLINE JOURNAL

Pacific Journal of Optimization
Vol. 10, No. 1, pp. 177–198, January 2014

MULTI-NETWORK COMBINED COOLING HEATING AND POWER SYSTEM SCHEDULING CONSIDERING EMISSION TRADING*

Hongming Yang, Dangqiang Zhang, Ke Meng
Zhao Yang Dong and Mingyong Lai

Abstract: A multi-network combined cooling heating and power (CCHP) system is composed of different energy resources and customer demand, which are connected by electricity network and heating/cooling pipe network. In this paper, the joint probability distribution of available power generation by multiple wind turbines is established based on Copula function and marginal prob-ability distribution of wind speed. The optimal scheduling model for multi-network CCHP system is proposed to reduce greenhouse gas emissions and maximize renewable energy utilization, meanwhile considering the impacts of emission trading scheme on fossil-fired units and security operation constraints of electricity network and heating/cooling pipe network. After that, sampling average approximation, function smoothing and global descent algorithm are employed in order to address the calculation of non-smooth and non-convex scheduling optimization problem. The global descent algorithm continuously updates the local optimal solutions to find global optimal solutions. Finally, one modified 15-bus system is used to analyze the impacts of joint probability distribution, sampling number and emission trading scheme on the scheduling results, which verify the effectiveness of the proposed model and solving algorithm.

Key words: *copula function, emissions trading, global descent algorithm, multi-network combined cooling heating and power system, optimal scheduling, renewable energy*

Mathematics Subject Classification: *Primary 93A49, 60-08; Secondary 00A78*

1 Introduction

Nowadays, due to the fossil fuel crisis contributed by explosive growth in energy demand, energy saving solutions has attracted widespread concerns. In order to reduce energy consumption, combined cooling heating and power (CCHP) systems have been widely deployed around the world. CCHP systems can generate electricity whilst recovering normally wasted thermal energy in an electricity generator, and then uses it for steam or hot water production, space heating or cooling [5]. By using a CCHP system, the fuel that would otherwise be used to produce heat or cold in a separate unit is saved. The most significant benefits of CCHP systems can be summarized as, a) supply electrical load meanwhile cover heating and cooling requirements during cold and hot sea-sons; b) reduce operating cost and life-cycle cost.

*This work was supported by the National Natural Science Foundation of China (Key Project 71331001, General Project 71071025) and the National Outstanding Youth Science Foundation of China (70925006).

In order to assist with the management of CCHP systems, extensive researches have been conducted to formulate operational strategies. A hybrid electric-thermal operational model is pro-posed in [6], which was a good alternative to the operation of CCHP system since it can yield good reduction of primary energy consumption and operational cost. An efficient algorithm is proposed to optimize the operation of a CCHP gas-motor-based system. The results indicate that optimal operation of CCHP system under the reasonable investment on power plant and equipment can be controlled [19]. In [10], an optimal operational strategy is proposed depending on an integrated performance criterion (IPC) considering the primary energy consumption, the operational cost. Then the operating point of CCHP system is located in a corresponding operating mode region to achieve improved IPC. In [20], uncertainties in CCHP system, such as thermal load, natural gas price and electricity price are considered in a representative model. Moreover, some solving algorithms have been developed for the scheduling of CCHP systems. In [21], a multi-objective approach based on evolutionary programming is applied to solve the economic operation problem of combined heating and power (CHP) systems. Genetic algorithm is also used to obtain operational strategy for a CHP system in [13]. In [2], particle swarm optimization is applied to schedule optimal operation of CHP systems. In the above studies, the security constraints of electricity network, heating network, and cooling network are ignored, which cannot guarantee the stable operation of multi-network CCHP systems.

The conventional CCHP systems are built on fossil fuels, including coal, oil, and natural gas. Unbridled use of fossil fuels is causing concerns of global warming and other environmental issues. The efficient utilization of renewable energy resources, such as wind and solar has been paid more attention. The optimal scheduling for the CCHP system based on fossil fuels and renewable energy resources has not been studied in detail. In addition, the increasing environmental challenges have forced power generation enterprises to modify their system operation routines to reduce greenhouse gas (GHG) emissions by exploiting clean energy [7]. In [23], the carbon tax is included in the operational cost to control GHG emissions. However, an important drawback of emission tax is that emission is not guaranteed to be limited to a specific cap. The cap-and-trade program seeks to control GHG emissions within specified limits by establishing tradable emission allowances. The tradable price of emission allowances provides an incentive to reduce emissions in the most cost-effective way [4]. This program has been adopted in the U.S. and the E.U.. Thus, it is necessary to investigate a better model for optimally scheduling the CCHP system based on fossil fuels and renewable energy resources under emission trading schemes.

Therefore, in this paper, a novel model is proposed to study optimal scheduling problem for multi-network CCHP systems under emission trading schemes, in order to minimize GHG emissions and maximize renewable energy utilization. The remarkable characteristics of the proposed framework can be summarized as follows: 1) fossil fuel based and renewable energy based electricity/heating/cooling generation is included; 2) the correlations among multiple renewable energy resources are considered; 3) the security constraints of electricity network and heating/cooling network are incorporated; 4) the CCHP optimal scheduling model under emission trading schemes is formulated. However, in order to accommodate the optimal scheduling strategies, more efficient algorithms should be developed. This paper is organized as follows, after introduction section a mathematical model of multi-network CCHP system is proposed. Then, an optimal scheduling model is proposed, which considers the uncertainties of renewable energy and emission trading price, and the security constraints of electricity network and heating/cooling pipe network. After that, sampling average approximation (SAA), function smoothing and global de-scent algorithm are employed to solve the optimization problem. One modified 15-bus system is used to verify the performance of the proposed model and solving algorithm. Conclusions and further developments are discussed in the last section.

2 Mathematical Model of Multi-Network CCHP System

2.1 Notation

In this section all symbols used in this paper are classified, into indices, parameters, decision variables and auxiliary functions.

Indices

i	The i-th CCHP unit.	fo	Fossil fuel.
N	Total number of units in the system.	re	Renewable energy.
M	Total sampling number in the SAA.	l	Transmission line.

Parameters

ϖ	Scheduling period [h].	$\eta_{i,fo,h}$	Conversion efficiency from fossil fuel to heat/cool energy.
$\eta_{i,fo,e}$	Conversion efficiency from fossil fuel to electrical energy.	$\eta_{i,fo,e,h}$	Conversion efficiency from fossil fuel to wasted thermal energy while generating electricity.
$\upsilon_{i,fo}$	Scheduling factor which represents the ratio of fossil fuel used for generating electricity	$\upsilon_{i,re}$	Scheduling factor which represents the ratio of renewable energy used for generating electricity.
$q_{i,fo}$	The amount of consumed fossil fuel by unit i [kg].	$q_{i,re}$	The amount of consumed renewable energy by unit i [kWh].
$v_{i,w}$	Wind speed [m/s].	$v_{i,w,in}$	The cut-in wind speed [m/s].
$v_{i,w,r}$	The rated wind speed [m/s].	$v_{i,w,out}$	The cut-out wind speed [m/s].
$v_{i,w,f}$	The predicted wind speed [m/s].	λ_i	Rayleigh distribution parameter.
$P_{i,w,r}$	The rated power of wind turbine [kW].	$P_{i,w,s}$	The available power output of wind turbine [kW].
$\hbar$	Smoothing parameter.	p_e	The price of purchasing electrical energy from adjacent system [\$/kWh].
p_h	The price of purchasing heat/cold energy from adjacent system [\$/MJ].	p_{et}	The price of emissions trading [\$/ton].
$\kappa_{i,fo,e}$	The pollutant emissions rate of electricity generation by fossil fuel [ton/kWh].	$\kappa_{i,fo,h}$	The pollutant emissions rate of heat/cold generation by fossil fuel [ton/MJ].
ι	The parameter of the Copula function.	B	The specific heat of water [MJ/(kg^0C)].
T_{i0}	Temperature of water in pipe network before heating/cooling [^0C].	T_i	Temperature of water in pipe net-work after heating/cooling [^0C].
D	The density of water [kg/m^3].	A	The pipeline area [m^2].
V_i	The flow rate of water [m/s]	$P_l^{\max}$	The upper limit of transmitted power of line l [kW].

$P_{i,L}$	The electrical load at node i [kWh].	$H_{i,L}$	The heat/cold load at node i [MJ].
$Q_{et,i}$	The amount of emissions [ton].	$Q^0_{et,i}$	The allocated initial emission allowances [ton].
$P_{i,re,s}$	The available electricity generation by renewable unit i [kWh].	$H_{i,re,s}$	The available heat/cold generation by renewable unit i [MJ].
$\underline{P_{i,fo}}$	The lower limits of electricity generation by fossil-fired unit i [kWh].	$\overline{P_{i,fo}}$	The upper limits of electricity generation by fossil-fired unit i [kWh].
$\underline{P_{i,re}}$	The lower limits of electricity generation by renewable unit i [kWh].	$\overline{P_{i,re}}$	The upper limits of electricity generation by renewable unit i [kWh].
$\underline{H_{i,fo}}$	The lower limits of heating/cooling generation by fossil-fired unit i [MJ].	$\overline{H_{i,fo}}$	The upper limits of heating/cooling generation by fossil-fired unit i [MJ].
$\underline{H_{i,re}}$	The lower limits of heating/cooling generation by renewable unit i [MJ].	$\overline{H_{i,re}}$	The upper limits of heating/cooling generation by renewable unit i [MJ].
$\underline{P_S}$	The lower limits of purchased electrical energy from adjacent system [kWh].	$\overline{P_S}$	The upper limits of purchased electrical energy from adjacent system [kWh].
$\underline{H_S}$	The lower purchased heat/cold energy from adjacent system [MJ].	$\overline{H_S}$	The upper purchased heat/cold energy from adjacent system [MJ].
$a_{i,fo,e}$	Linear fuel cost coefficients of electricity generation by fossil-fired unit i [$/kWh].	$b_{i,fo,e}$	Quadratic fuel cost coefficients of electricity generation by fossil-fired unit i [$\$/kW^2h$].
$a_{i,fo,h}$	Linear fuel cost coefficients of heat/cold generation by fossil-fired unit i [$/MJ].	$b_{i,fo,h}$	Quadratic fuel cost coefficients of heat/cold generation by fossil-fired unit i [$\$/MJ^2$].
$c_{i,fo,e}$	Linear operation cost coefficients of electricity generation by fossil-fired unit i [$/kWh].	$c_{i,fo,h}$	Linear operation cost coefficients of heat/cold generation by fossil-fired unit i [$/MJ].
$c_{i,re,e}$	Linear operation cost coefficients of electricity generation by renewable unit i [$/kWh].	$c_{i,re,h}$	Linear operation cost coefficients of heat/cold generation by renewable unit i [$/MJ].
$c^u_{i,re,e}$	Linear underestimation penalty cost coefficients of electricity generation by renewable unit i [$/kWh].	$c^o_{i,re,e}$	Linear overestimation penalty cost coefficients of electricity generation by renewable unit i [$/kWh].
$c^u_{i,re,h}$	Linear underestimation penalty cost coefficients of heat/cold generation by renewable unit i [$/MJ].	$c^o_{i,re,h}$	Linear overestimation penalty cost coefficients of heat/cold generation by renewable unit i [$/MJ].
χ_{li}	Sensitivity coefficients of injected power at node. i with respect to transmitted power of line l.		

Decision Variables

$P_{i,fo}$	Electricity generated by fossil-fired unit i [kWh].
$P_{i,re}$	Electricity generated by renewable energy unit i [kWh].
P_S	Electricity purchased from adjacent main system [kWh].
$P_{i,w}$	Electricity generated by wind unit i [kW].
$H_{i,fo}$	Heat/cool energy produced by fossil-fired unit i [MJ].
$H_{i,re}$	Heat/cool energy produced by renewable energy unit i [MJ].
H_S	Heat/cold energy purchased from adjacent main system [MJ].

Auxiliary Functions

Π	Total system cost [$].
$E[\cdot]$	Expectation operator.
$[\cdot]^+$	Operator $[g(y)]^+ = \max\{0, g(y)\}$.
$\delta(\cdot)$	Dirac Delta function.
$erf(\cdot)$	Gaussian error function.
$\rho_{i,w}(\cdot)$	Probability density function of wind speed.

2.2 Multi-Network CCHP System

Generally, a normal CCHP system is composed of several units, which are connected by electricity network and heating/cooling pipe network. The structure of a typical three-unit CCHP system is shown in Fig. 1.

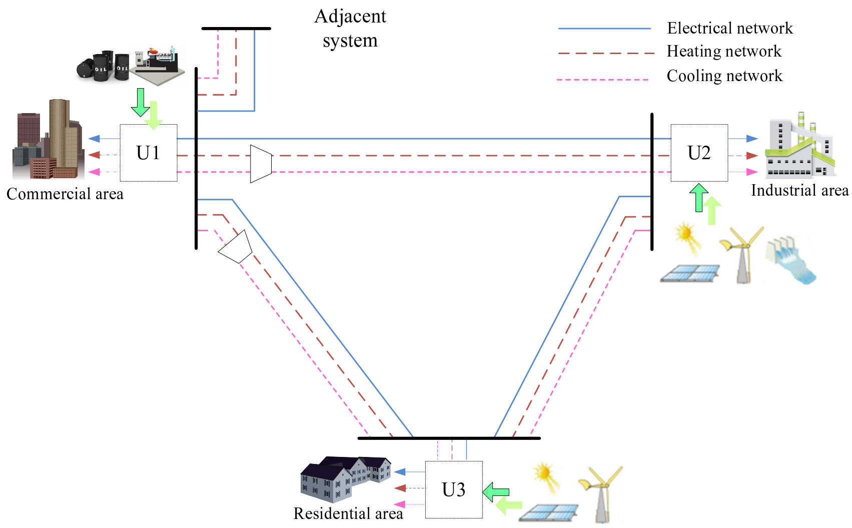

Figure 1: The structure of a typical three-unit CCHP system

A multi-network CCHP system is composed of coal, wind, solar and other primary energy resources, which can produce electrical/heat/cold energy simultaneously. The produced energy can be connected to system through electricity network and heating/cooling pipe network, in order to meet the electrical load as well as demand for heating and cooling. The inputs and outputs are shown in Fig. 2.

In Fig. 2, the fossil fuel based CCHP conversion system produces the electrical/heat/cool energy. The CCHP unit can generate electricity whilst recovering wasted thermal energy for hot water production, space heating or cooling. Thus, in a scheduling period, the conversion

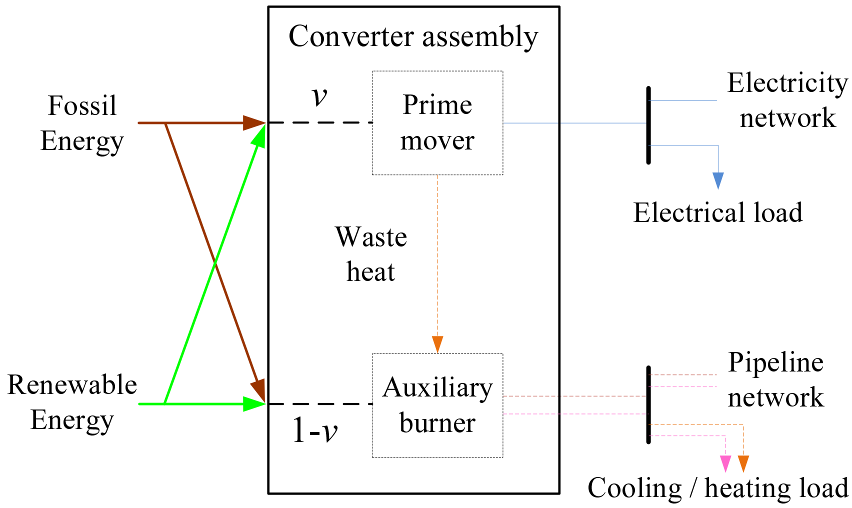

Figure 2: Inputs and outputs of a CCHP unit

relationship between electrical/heat/cool energy and the fossil fuel can be expressed as [12]

$$P_{i,fo} = \upsilon_{i,fo} \cdot \eta_{i,fo,e} \cdot q_{i,fo}, \tag{2.1}$$

$$H_{i,fo} = (1 - \upsilon_{i,fo}) \cdot \eta_{i,fo,h} \cdot q_{i,fo} + \upsilon_{i,fo} \cdot \eta_{i,fo,e} \cdot \eta_{i,fo,e.h} \cdot q_{i,fo}. \tag{2.2}$$

Simultaneously, the renewable energy based CCHP conversion system also produces electrical/heat/cool energy. After generating electricity, the CCHP unit can also use wasted thermal energy for heating/cooling. The conversion relationship between electrical/heat/cold energy and available renewable energy can be expressed as

$$P_{i,re,s} = f_{i,re,e}\left(\upsilon_{i,re} \cdot q_{i,re}\right), \tag{2.3}$$

$$H_{i,re,s} = f_{i,re,h}\left[(1 - \upsilon_{i,re}) \cdot q_{i,re}\right] + f_{i,re,e,h}\left(\upsilon_{i,re} \cdot q_{i,re}\right). \tag{2.4}$$

where,$f_{i,re,e}(\cdot)$, $f_{i,re,h}(\cdot)$ are CCHP conversion functions from renewable energy to electrical energy and heat/cool energy, respectively; $f_{i,re,e,h}(\cdot)$ represents the CCHP conversion functions from wasted thermal energy after generating electricity to heat/cool energy.

2.3 Renewable Energy Based CCHP Conversion System

Take wind power as an example, due to low conversion efficiency from wind energy into heat/cool energy, in this paper, wind energy is only used for electricity generation. The available power output of wind turbine can be expressed as a function of wind speed

$$P_{i,w,s} = \begin{cases} 0 & v_{i,w} < v_{i,w,in}, v_{i,w} > v_{i,w,out} \\ k_{i,w}v_{i,w} + d_{i,w} & v_{i,w,in} \le v_{i,w} \le v_{i,w,r} \\ P_{i,w,r} & v_{i,w,r} < v_{i,w} \le v_{i,w,out} \end{cases}, \tag{2.5}$$

where $k_{i.w}$ and $d_{i.w}$ are parameters which can be calculated as

$$\begin{cases} k_{i,w} = \frac{P_{i,w,r}}{v_{i,w,r} - v_{i,w,in}} \\ d_{i,w} = -\frac{v_{i,w,in}P_{i,w,r}}{v_{i,w,r} - v_{i,w,in}} \end{cases}. \tag{2.6}$$

An extensive review of various probability density function (PDF) of wind speed was provided in [3, 8], and comparisons were made. The results indicated that Rayleigh or Weibull distribution is the widely accepted model. In this paper, it is assumed that wind speed follows Rayleigh distribution, its PDF is

$$\rho_{i,w}\left(v_{i,w}\right) = \frac{v_{i,w}}{\lambda_i^2} \exp\left(-\frac{v_{i,w}^2}{2\lambda_i^2}\right), \tag{2.7}$$

where λ_i is distribution parameter and meets the following relationship [24]

$$\lambda_i = v_{i,w,f} \Big/ \sqrt{\pi/2}. \tag{2.8}$$

The empirical distribution of wind speed and fitted theoretical distribution are shown in Fig. 3. It can be seen that Rayleigh distribution can well fit the stochastic characters of wind speed.

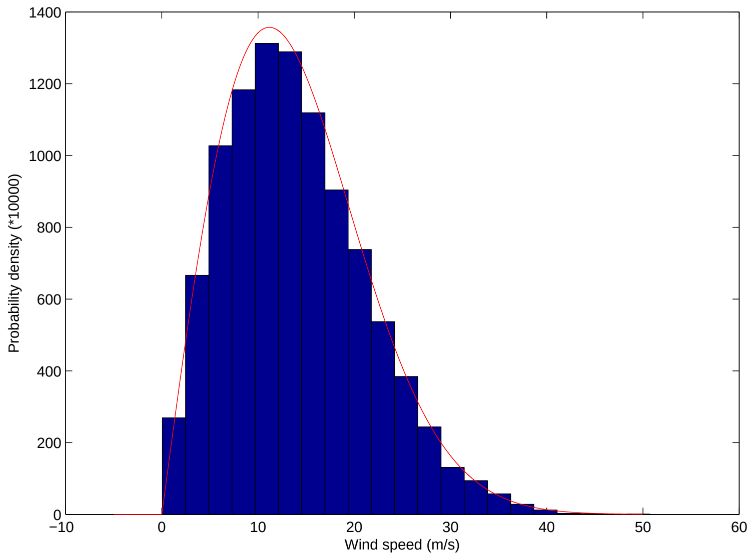

Figure 3: Empirical and theoretical distribution of wind speed

According to (2.5), three portions of available wind power output can be analyzed and the corresponding PDF can be calculated based on the available wind turbine power output curve and wind speed PDF, respectively.

(1) For $0 < P_{i,w,s} < P_{i,w,r}$,

$$\rho_{i,w}\left(P_{i,w,s}\right) = \frac{P_{i,w,s} - d_{i,w}}{\lambda_i^2 k_{i,w}^2} \exp\left[\frac{\left(P_{i,w,s} - d_{i,w}\right)^2}{-2\lambda_i^2 k_{i,w}^2}\right]. \tag{2.9}$$

(2) For $P_{i,w,s} = 0$,

$$\rho_{i,w}\left(P_{i,w,s}\right) = \left[1 - \exp\left(-\frac{v_{i,w,in}^2}{2\lambda_i^2}\right) + \exp\left(-\frac{v_{i,w,out}^2}{2\lambda_i^2}\right)\right] \delta\left(P_{i,w,s}\right). \tag{2.10}$$

(3) For $P_{i,w,s} = P_{i,w,r}$,

$$\rho_{i,w}\left(P_{i,w,s}\right) = \left[\exp\left(-\frac{v_{i,w,r}^2}{2\lambda_i^2}\right) - \exp\left(-\frac{v_{i,w,out}^2}{2\lambda_i^2}\right)\right]\delta\left(P_{i,w,s} - P_{i,w,r}\right). \tag{2.11}$$

Based on (2.9)-(2.11), the probability distribution function of available wind power output is expressed as

$$F_i\left(P_{i,w,s}\right) = \begin{cases} 1 - \exp\left(-\frac{v_{i,w,in}^2}{2\lambda_i^2}\right) + \exp\left(-\frac{v_{i,w,out}^2}{2\lambda_i^2}\right), & P_{i,w,s} = 0 \\ 1 + \exp\left(-\frac{v_{i,w,out}^2}{2\lambda_i^2}\right) - \exp\left(-\frac{v_{i,w}^2}{2\lambda_i^2}\right), & 0 < P_{i,w,s} < P_{i,w,r} \\ 1, \quad P_{i,w,s} = P_{i,w,r} \end{cases}. \tag{2.12}$$

The available wind power output of different wind turbines within a distribution system can be correlated since they draw power from an identical wind source. To model this correlation, the Copula function is employed. The probability distributions of available wind power of N wind turbines are $F_1\left(P_{1,w,s}\right), \cdots, F_N\left(P_{N,w,s}\right)$, respectively, as calculated in (2.12), then there exist a Copula function $C(\cdot)$ such that the joint distribution $\Re(\cdot)$ can be expressed as [9, 22]

$$\Re\left(P_{1,w,s}, \cdots, P_{N,w,s}\right) = C\left[F_1\left(P_{1,w,s}\right), \cdots, F_N\left(P_{N,w,s}\right)\right]. \tag{2.13}$$

Although there are several different types of Copula functions, the Gumbel-Copula function is unsymmetrical and upper fat-tailed, which well matches the characteristics of available wind power correlation [1]; it is employed to model the joint distribution of available wind power outputs of multiple wind turbines, i.e.

$$\Re\left(P_{1,w,s}, \cdots, P_{N,w,s}\right) = \exp\left\{-\left[\left(-InF_1\left(P_{1,w,s}\right)\right)^{\iota} + \cdots + \left(-InF_N\left(P_{N,w,s}\right)\right)^{\iota}\right]^{\frac{1}{\iota}}\right\}, \tag{2.14}$$

where parameter ι can be estimated using the MLE method.

3 Optimal Scheduling Model for Multi-Network CCHP System Considering Emission Trading

In the optimal scheduling model for multi-network CCHP system, the decision variables include electrical/heat/cold energy generated by fossil fuel; electrical/heat/cold energy generated by renewable energy (e.g. wind energy), and electrical/heat/cold energy purchased from adjacent system, considering the impacts of emission trading schemes. The objective is to minimize the total system cost and maximize the penetration of renewable energy under the security constraints of electricity network and heating/cooling pipe network. The optimal scheduling model for multi-network CCHP system considering emission trading is proposed in this section.

3.1 Objective Function

The objective function of the optimal scheduling model, is composed of production cost Π_1 of electrical/heat/cold by fossil fuel and renewable units, purchase cost Π_2 of electrical/heat/cold energy from adjacent system, overestimation/underestimation cost Π_3 of renewable energy, and emission trading cost Π_4. It can been expressed as

$$\underset{P_{i,re},P_{i,fo},H_{i,re},H_{i,fo},P_S,H_S}{Min} E[\Pi] = E[\Pi_1] + E[\Pi_2] + E[\Pi_3] + E[\Pi_4]. \tag{3.1}$$

1) Production Cost of Electrical/heat/cold Energy

   Production cost of electrical/heat/cold energy includes fuel cost Π_{11}, operation cost Π_{12}. In this paper, start-up and shunt-down cost of conventional units are ignored, and the fuel cost of renewable energy is set as zero. It is assumed that the fuel cost functions for producing both electrical energy and heat/cold energy are quadratic and their operation cost functions are linear [14]. Thus, Π_{11} and Π_{12} can be calculated as

$$\Pi_{11} = \sum_i \sum_{fo} \begin{bmatrix} a_{i,fo,e} P_{i,fo} + b_{i,fo,e} P_{i,fo}^2 + a_{i,fo,h} \left(H_{i,fo} - \eta_{i,fo,e.h} P_{i,fo} \right) \\ + b_{i,fo,h} (H_{i,fo} - \eta_{i,fo,e.h} P_{i,fo})^2 \end{bmatrix}, \tag{3.2}$$

$$\Pi_{12} = \sum_i \begin{bmatrix} \sum\limits_{fo} [c_{i,fo,e} P_{i,fo} + c_{i,fo,h} \left(H_{i,fo} - \eta_{i,fo,e.h} P_{i,fo} \right)] + \\ \sum\limits_{re} [c_{i,re,e} P_{i,re} + c_{i,re,h} \left(H_{i,re} - \eta_{i,re,e.h} P_{i,re} \right)] \end{bmatrix}. \tag{3.3}$$

2) Purchase Cost of Electrical/heat/cold Energy from Adjacent System

   The CCHP system is connected to adjacent system. When the electrical/heat/cold energy is not sufficient to its loads in the CCHP system, the energy can be purchased from the adjacent system. The purchase cost is expressed as

$$\Pi_2 = p_e P_S + p_h H_S. \tag{3.4}$$

   If the electrical/heat/cold energy P_S, H_S are negative, it represents the injection from CCHP to the adjacent system, and Π_2 represents negative cost (i.e. benefit).

3) Overestimation/Underestimation Cost of Renewable Energy

   Due to the uncertainty of renewable energy, the predictions normally have some errors. The underestimation and overestimation penalty costs are introduced to maximize the penetration of renewable energy. The underestimation situation occurs if the actual generated power is more than the available power output, thus the system operator should compensate for the surplus power. On the other hand, if the actual power is less than the available power output, the operator needs to purchase power from an alternate source and pay the overestimation cost. These two penalty costs are assumed as [24]

$$\Pi_3 = \sum_i \sum_{re} \begin{pmatrix} c_{i,re,e}^u [P_{i,re,s} - P_{i,re}]^+ + c_{i,re,e}^o [P_{i,re} - P_{i,re,s}]^+ + \\ c_{i,re,h}^u [H_{i,re,s} - H_{i,re}]^+ + c_{i,re,h}^o [H_{i,re} - H_{i,re,s}]^+ \end{pmatrix}. \tag{3.5}$$

   When considering a single wind farm or multiple wind farms with independent probabilistic characteristics, based on the PDF of available power output in (2.12) by wind turbine, the expectation of penalty cost can be expressed analytically. The expectation of underestimate penalty cost by wind energy is

$$\begin{aligned} & E\left(c_{i,we}^u \varpi \left[P_{i,w,s} - P_{i,w} \right]^+ \right) \\ & = c_{i,we}^u \varpi \left(P_{i,w,r} - P_{i,w} \right) \left[\exp\left(-\frac{v_{i,w,r}^2}{2\lambda_i^2} \right) - \exp\left(-\frac{v_{i,w,out}^2}{2\lambda_i^2} \right) \right] \\ & \quad - c_{i,we}^u \varpi \left(P_{i,w,r} - P_{i,w} \right) \cdot \left[\exp\left(-\frac{(P_{i,w,r} - d_{i,we})^2}{2\lambda_i^2 k_{i,we}^2} \right) \right] \\ & \quad + \frac{\sqrt{2\pi} \lambda_i c_{i,we}^u \varpi k_{i,we}}{2} \left[erf\left(\frac{P_{i,w,r} - d_{i,we}}{\sqrt{2} \lambda_i k_{i,we}} \right) - erf\left(\frac{P_{i,w} - d_{i,we}}{\sqrt{2} \lambda_i k_{i,we}} \right) \right] \end{aligned}, \tag{3.6}$$

The expectation of overestimate penalty cost by wind energy is

$$\begin{array}{l} E\left(c_{i,we}^{o}\varpi\left[P_{i,w}-P_{i,w,s}\right]^{+}\right) \\ =c_{i,we}^{o}\varpi P_{i,w}\left[1-\exp\left(-\frac{v_{i,w,in}^{2}}{2\lambda_{i}^{2}}\right)+\exp\left(-\frac{v_{i,w,out}^{2}}{2\lambda_{i}^{2}}\right)\right] \\ +c_{i,we}^{o}\varpi P_{i,w}\exp\left(-\frac{d_{i,we}^{2}}{2\lambda_{i}^{2}k_{i,we}^{2}}\right) \\ -\frac{\sqrt{2\pi}\lambda_{i}c_{i,we}^{o}\varpi k_{i,we}}{2}\cdot\left[erf\left(\frac{P_{i,w}-d_{i,we}}{\sqrt{2}\lambda_{i}k_{i,we}}\right)-erf\left(\frac{-d_{i,we}}{\sqrt{2}\lambda_{i}k_{i,we}}\right)\right] \end{array}. \tag{3.7}$$

When considering the probability correlation of different renewable energy resources subjecting to similar weather conditions, the mathematical form of Copula function in (2.14) becomes complex and the expectations of overestimation and underestimation costs cannot be expressed analytically. Therefore, the SAA method [11] is applied to calculate the expectation functions in (3.5), i.e.

$$E\left[\Pi_{3}\right]=\frac{1}{M}\sum_{i}\sum_{re}\sum_{m=1}^{M}\left(\begin{array}{l} c_{i,re,e}^{u}\left[P_{i,re,s}^{(m)}-P_{i,re}\right]^{+}+c_{i,re,e}^{o}\left[P_{i,re}-P_{i,re,s}^{(m)}\right]^{+}+ \\ c_{i,re,h}^{u}\left[H_{i,re,s}^{(m)}-H_{i,re}\right]^{+}+c_{i,re,h}^{o}\left[H_{i,re}-H_{i,re,s}^{(m)}\right]^{+} \end{array}\right). \tag{3.8}$$

where m represents a sampling in the SAA.

4) Emission Trading Cost In the emission trading scheme, each CCHP unit should comply with its emissions obligation. The amount of emission allowances purchased by each CCHP unit is equal to the difference between its aggregate emissions burden and the allowed emissions amount [14]. The emissions burden of each CCHP unit when producing electrical/heat/cool energy can be calculated by

$$Q_{et,i}=\sum_{fo}\left[\kappa_{i,fo,e}P_{i,fo}+\kappa_{i,fo,h}\left(H_{i,fo}-\eta_{i,fo,e.h}\cdot P_{i,fo}\right)\right]. \tag{3.9}$$

Thus, the purchasing cost of emission allowances is

$$\Pi_{4}=\sum_{i}p_{et}\cdot\left(Q_{et,i}-Q_{et,i}^{0}\right). \tag{3.10}$$

If the emissions burden is less than the allowed emissions amount, it means the sale of emission allowances from CCHP unit to the emission trading market, and Π_4 represents negative cost (i.e. benefit). Considering the uncertainty of emission allowances price in the market, it is assumed that p_{et} follows the normal distribution with mean μ_{et} and variance σ_{et}. Thus, the expectation of emission trading cost is

$$E\left(\Pi_{4}\right)=E\left[\sum_{i}p_{et}\left(Q_{et,i}-Q_{et,i}^{0}\right)\right]=\mu_{et}\sum_{i}\left(Q_{et,i}-Q_{et,i}^{0}\right). \tag{3.11}$$

3.2 Constraints

According to the actual requirements of secure and economic operation of multi-network CCHP systems, the system constraints should be considered, including the balance of electrical/heat/cool supply and demand, security constraints of electricity network and heating/cooling pipe network, and electrical/heat/cool output limits of CCHP units.

1) The Balance of Electrical/heat/cool Supply and Demand

$$\left\{ \begin{array}{l} \sum\limits_{i} \left(\sum\limits_{fo} P_{i,fo} + \sum\limits_{re} P_{i,re} \right) + P_S = \sum\limits_{i} P_{i,L} \\ \sum\limits_{i} \left(\sum\limits_{fo} H_{i,fo} + \sum\limits_{re} H_{i,re} \right) + H_S = \sum\limits_{i} H_{i,L} \end{array} \right. . \tag{3.12}$$

2) Security Constraints of Electricity Network

$$-P_l^{\max} \leq \sum_{i} \frac{\chi_{il}}{\varpi} \left(\sum_{fo} P_{i,fo} + \sum_{re} P_{i,re} - P_{i,L} \right) \leq P_l^{\max}. \tag{3.13}$$

3) Security constraints of Heating/cooling Pipe Network

In order to simplify pipe network, it is assumed that the heating/cooling pipes are radial, as shown in Fig. 4.

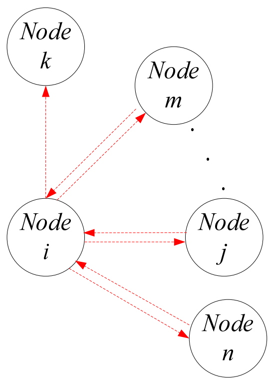

Figure 4: Radial heating/cooling pipe network

There are two types of transmission situations in heating/cooling pipes. One type, the heat/cool energy is bidirectionally transferred between nodes i and j. Another type, the heat/cool energy is unidirectionally transferred when the load node only consumes heat/cold energy. According to thermodynamic equation, the fluid temperature is increased by absorbing heat can be computed by

$$\sum_{fo} H_{i,fo} + \sum_{re} H_{i,re} - H_{i,L} = BDAV_i \left(T_i - T_{i0} \right), \tag{3.14}$$

where fluid speed V_i should satisfied

$$-V_i^{\max} \leq \frac{\sum\limits_{fo} H_{i,fo} + \sum\limits_{re} H_{i,re} - H_{i,L}}{BDA \left(T_i - T_{i0} \right)} = V_i \leq V_i^{\max} \ \ \forall i. \tag{3.15}$$

4) Constraints of CCHP Units

The electrical/heat/cool output limits of fossil fuel and renewable energy based CCHP units should be satisfied, i.e.

$$\underline{P_{i,fo}} \le P_{i,fo} \le \overline{P_{i,fo}}, \quad \underline{P_{i,re}} \le P_{i,re} \le \overline{P_{i,re}}, \quad \forall i, fo, re, \tag{3.16}$$

$$\underline{H_{i,fo}} \le H_{i,fo} \le \overline{H_{i,fo}}, \quad \underline{H_{i,re}} \le H_{i,re} \le \overline{H_{i,re}}, \quad \forall i, fo, re, \tag{3.17}$$

$$\underline{P_S} \le P_S \le \overline{P_S}, \quad \underline{H_S} \le H_S \le \overline{H_S}. \tag{3.18}$$

4 Global Descent Algorithm Based Optimal Scheduling Solver

4.1 Function Smoothing Transformation

From the optimal scheduling model for multi-network CCHP system in (3.1)-(3.18), we can find that the objective function $E[\Pi]$ is a non-smooth function due to non-smooth term $[\cdot]^+$ (the function at point $(0,0)$ is not smoothened) in the overestimation/underestimation cost. It is processed by smoothing method [18]. Denote

$$g'(y) = [g(y)]^+ = \max\{0, g(y)\}. \tag{4.1}$$

Then, its smoothing function is

$$g_\hbar(y) = \hbar \ln\left\{1 + \exp\left[\frac{g(y)}{\hbar}\right]\right\}, \tag{4.2}$$

where smoothing parameter $\hbar$ is taken as a small positive number.

Thus, by using (4.2), the non-smooth cost function in (3.8) is reformulated as the following smoothing function.

$$E[\Pi_3] = \frac{\hbar}{M}\sum_i\sum_{re}\sum_{m=1}^{M}\begin{pmatrix} c^u_{i,re,e}\ln\left\{1+\exp\left[\frac{P^{(m)}_{i,re,s}-P_{i,re}}{\hbar}\right]\right\}+ \\ c^o_{i,re,e}\ln\left\{1+\exp\left[\frac{P_{i,re}-P^{(m)}_{i,re,s}}{\hbar}\right]\right\}+ \\ c^u_{i,re,h}\ln\left\{1+\exp\left[\frac{H^{(m)}_{i,re,s}-H_{i,re}}{\hbar}\right]\right\}+ \\ c^o_{i,re,h}\ln\left\{1+\exp\left[\frac{H_{i,re}-H^{(m)}_{i,re,s}}{\hbar}\right]\right\} \end{pmatrix}. \tag{4.3}$$

The reformulated optimal scheduling model discussed above is a non-convex, but smoothed optimization problem.

4.2 Global Descent Solving Algorithm

For the non-convex smoothing optimization problem, some traditional solving algorithms (e.g. interior point algorithm) can only get local optimal solutions. In order to obtain the global optimal solution, a global descent algorithm is introduced [17]. For simplicity, the optimization problem for multi-network CCHP system can be expressed as

$$\underset{\mathbf{x}}{Min}\ f(\mathbf{x}) = E[\Pi], \tag{4.4}$$

$$s.t.\quad h(\mathbf{x}) = 0\ ,\ g(\mathbf{x}) \le 0. \tag{4.5}$$

where $\mathbf{x} = [P_{i,fo}, H_{i,fo}, P_{i,re}, H_{i,re}, P_S, H_S]^T$ is a vector composed of all decision variables; $f(\cdot)$ represents the objective function in the optimal model; $h(\cdot), g(\cdot)$ represents the equality and inequality constraints, respectively.

In this paper, the primal-dual interior point algorithm is applied to find the local optima solution $\hat{\mathbf{x}}^{(k)}$ of this model (4.4)-(4.5), and then the two-parameter global descent function is introduced [17], which can be represented as

$$G_{\varsigma,\theta,\hat{\mathbf{x}}^{(k)}}(\mathbf{x}) = \left[f(\mathbf{x}) - f\left(\hat{\mathbf{x}}^{(k)}\right)\right] \cdot V_\varsigma\left[f(\mathbf{x}) - f\left(\hat{\mathbf{x}}^{(k)}\right)\right] - \theta\left\|\mathbf{x} - \hat{\mathbf{x}}^{(k)}\right\|, \tag{4.6}$$

where $\theta > 0$, $0 < \varsigma < 1$; and the function $V_\varsigma(\cdot)$ is

$$V_\varsigma\left[f(\mathbf{x}) - f\left(\hat{\mathbf{x}}^{(k)}\right)\right] = \varsigma \cdot \left[(1-r)\left(\frac{\varsigma - r\varsigma}{1 - r\varsigma}\right)^{\left[f(\mathbf{x}) - f\left(\hat{\mathbf{x}}^{(k)}\right)\right]/\tau} + r\right], \tag{4.7}$$

where, $0 < r < 1$; $\tau > 0$ is an enough small positive number, which satisfies the following ine-quality constraint

$$0 < \tau < \min\left\{|f^* - f^{**}| : f^*, f^{**} \in f^*_{all}, f^* \neq f^{**}\right\}, \tag{4.8}$$

where, f^*_{all} is all the local optimal solutions, f^* and f^{**} are the two elements of f^*_{all}.

Generate a set of initial points, i.e. $\left\{\mathbf{x}^{(j)} \in \mathbf{X} \backslash N_\varepsilon\left(\hat{\mathbf{x}}^{(k)}\right) : j = 1, 2, \cdots, It\right\}$ where X is the feasible region of decision variable x; $N_\varepsilon\left(\hat{\mathbf{x}}^{(k)}\right)$ is the ε neighbor region of $\hat{\mathbf{x}}^{(k)}$. Set the current iterative point $\mathbf{x}_{cur} := \mathbf{x}^{(j)}$. If the following criterion is satisfied by

$$\left\|\nabla G_{\varsigma,\theta,\hat{\mathbf{x}}^{(k)}}(\mathbf{x}_{cur})\right\| < k_{small} \quad or \quad \left(\mathbf{x}_{cur} - \hat{\mathbf{x}}^{(k)}\right)^T \nabla G_{\varsigma,\theta,\hat{\mathbf{x}}^{(k)}}(\mathbf{x}_{cur}) \geq 0, \tag{4.9}$$

then adjust parameter ς such that global descent function satisfies

$$\left\|\nabla G_{\varsigma,\theta,\hat{\mathbf{x}}^{(k)}}(\mathbf{x}_{cur})\right\| \geq k_{small} \quad or \quad \left(v - \hat{\mathbf{x}}^{(k)}\right)^T \nabla G_{\varsigma,\theta,\hat{\mathbf{x}}^{(k)}}(\mathbf{x}_{cur}) < 0, \tag{4.10}$$

where k_{small} is an enough small positive number.

Then, based on a descent direction of $G_{\varsigma,\theta,\hat{\mathbf{x}}^{(k)}}$, the decision variables can be adjusted by

$$\mathbf{x}_{cur} := \mathbf{x}_{cur} - step \nabla G_{\varsigma,\theta,\mathbf{x}^*}(\mathbf{x}_{cur}), \tag{4.11}$$

where *step* is the step size of line search method, and the maximum step size can be calculated in [16]. If new decision variable $\mathbf{x}_{cur}$ satisfies

$$f(\mathbf{x}_{cur}) < f\left(\hat{\mathbf{x}}^{(k)}\right), \tag{4.12}$$

then $\mathbf{x}_{cur}$ is the transitional point of optimization problem. Stating from this point, the primal-dual interior point algorithm will be used to search new local optimal solution $\hat{\mathbf{x}}^{(k+1)}$, and repeat the above searching process. If $\mathbf{x}_{cur}$ starting from the initial points $\left\{\mathbf{x}^{(j)} : j = 1, 2, \cdots, It\right\}$ satisfies

$$f(\mathbf{x}_{cur}) \geq f\left(\hat{\mathbf{x}}^{(k)}\right), \tag{4.13}$$

the algorithm is incapable of finding a solution better than the current solution $\hat{\mathbf{x}}^{(k)}$, and $\hat{\mathbf{x}}^{(k)}$ is taken as a global optimal solution.

Table 1: Parameters of wind turbines

Bus	8	15
Operation Cost Coefficient	4.20	4.28
Underestimation Coefficient	3.0	3.0
Underestimation Coefficient	7.0	7.0
Rated Power	100	100
Cut-in Speed	5	5
Cut-out Speed	45	45
Rated Speed	15	15

5 Case Study

5.1 CCHP System Data

The proposed optimal scheduling model and its solving algorithm are tested with the 15-bus system [15] as shown in Fig. 5. The benchmark system consists of 5 CCHP units and 11

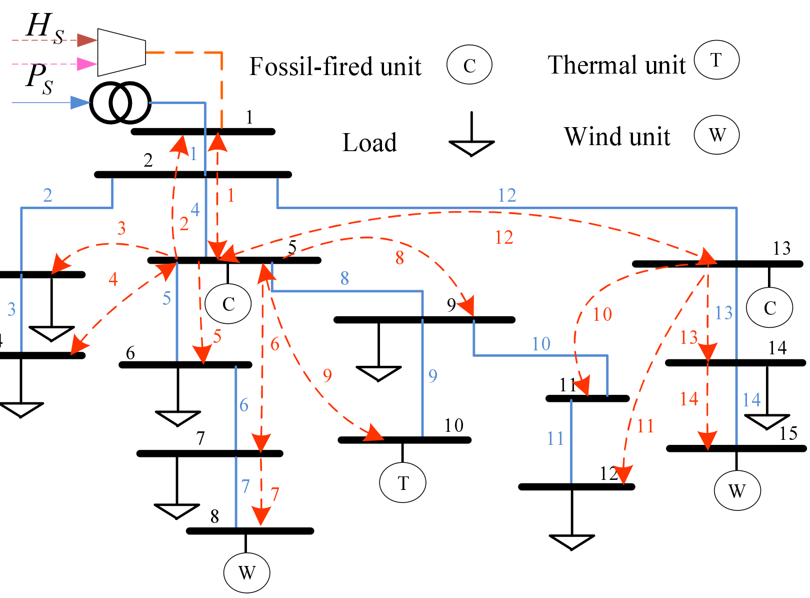

Figure 5: The structure of CCHP system

loads. Two wind power units are located at bus 8 and bus 15; thermal generation unit is located at bus 10; and two fossil-fired CCHP units are located at bus 5 and bus 13; and bus 5 is the central point of pipe network. The parameters of wind turbines are given in Table 1. The fuel cost coefficients and output limits, locations of CCHP units are shown in Table 2, and the demand at each bus is shown in Table 3. The parameters of electricity network and pipe network are given in Tables 4 and 5.

For the wind turbines in Table 1, according to (2.6), parameters $k_w = 10$ and $d_w = -50$. Sup-pose the forecasted wind speed in the study is 20m/s, then distribution parameter $\lambda =$

Table 2: Parameters of CCHP systems

Bus		a	b	c	η	$\eta_{fo,e,h}$	$\underline{P}/\underline{H}$	$\overline{P}/\overline{H}$	κ	Q_{et}^{0}
5	P	1.0	0.02	1.1	0.7	0.21	0	250	0.40	100
	H	1.0	0.02	1.0	0.7	-	0	300	0.5	
10	P	-	-	-	-	-	-	-	-	60
	H	1.3	0.04	1.5	0.6	-	0	100	0.70	
13	P	1.2	0.02	1.1	0.6	0.23	0	200	0.60	100
	H	1.1	0.03	1.1	0.6	-	0	200	0.55	

Table 3: The electrical/heat/cold energy demand

Bus	Electrical Load	Heat/Cold Load	Bus	Electrical Load	Heat/Cold Load
1	0	0	9	35	30
2	30	25	10	30	32
3	30	33	11	30	33
4	30	30	12	40	30
5	45	47	13	35	31
6	50	40	14	35	30
7	45	50	15	28	25
8	45	50			

15.9577; the prices of electricity and heat/cold energy are 7\$/kWh and 11\$/MJ, respectively; for the probability distribution of emission trading price, the mean is $\mu_0 = 6$, the variance is 1.3. The scheduling period is $\varpi = 1h$.

Table 4: The electrical/heat/cold energy demand

Transmission Line No.	1	2	3	4	5	6	7
Power Flow Limit	233	45	40	130	60	70	50
Transmission Line No.	8	9	10	11	12	13	14
Power Flow Limit	120	85	80	80	70	50	42

5.2 The Joint Probability Distribution of Two Wind Turbine Outputs

The wind speed data of wind turbines at buses 8 and 15 come from the real-world data of two wind farms (De Bilt and Soesterberg wind farms) in Netherlands (see http://www.knmi.nl/samenw/hydra). Based on (2.12), the joint probability distribution of two wind turbines is illustrated in Fig.6. As seen clearly, the outputs of the two wind turbines are highly correlated, and the joint probability distribution exhibits strong upper fat-tail effect. The Copula function is employed to model the correlation between two wind turbines.

To prove that the Gumbel-Copula function can well approximate the joint distribution of multiple wind turbine outputs, the quantile-quantile (QQ) plots are employed to compare five Copula functions and the joint distribution without considering the correlation between

Table 5: Parameters of heat/cool pipe network

Heat/cool Pipe Line No.	1	2	3	4	5	6	7
Flow Velocity Limit	21.7	4.2	3.9	12.2	5.6	6.5	4.7
Heat/cool Pipe Line No.	8	9	10	11	12	13	14
Flow Velocity Limit	11.4	8.2	7.4	7.3	6.6	4.8	4.0

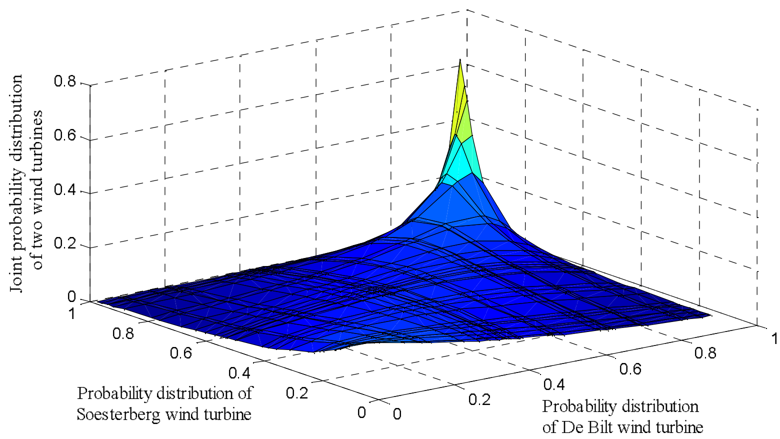

Figure 6: Joint probability distribution of two wind turbines

two wind power outputs, as shown in Fig.7. As shown in Fig.7, the Gumbel-Copula function can better model the tail correlation between multiple wind power outputs.

5.3 Performance of Global Descent Algorithm

Based on the primal-dual interior point algorithm, the global descent algorithm is employed to solve the optimal scheduling problem of CCHP system. Table 6 illustrates the result accuracy and calculation time by the global descent algorithm and only by the primal-dual interior point algorithm, where the sampling number of SAA is set as 5000; the smoothing parameter $\hbar$ is set as 0.0001. The convergence criterion of interior point algorithm is defined as the variation of the decision variables between two adjacent iterations is less than ε, i.e. $\left\|\mathbf{x}^{(k+1)} - \mathbf{x}^{(k)}/\mathbf{x}_{rate}\right\|_\infty \le \varepsilon$, where is the rated power of decision variables. In the interior point algorithm, $\mathbf{x}_{rate}$ is set as 10^{-6}, the calculation time is 15.522s. In the global descent algorithm, ε is set as 10^{-4}, each calculation time of local search by the interior point algorithm is less than 1s. The integration of local search and global search provides better solution and faster convergence rate (i.e. calculation time) than the interior point algorithm. Thus, for the nonlinear optimization problem, the global descent algorithm has better performance than the primal-dual interior point algorithm.

5.4 Optimal Scheduling Results Analysis

1) The Impact of Probability Distribution

Based on the Gumbel-Copula joint probability distribution of two wind turbines at buses

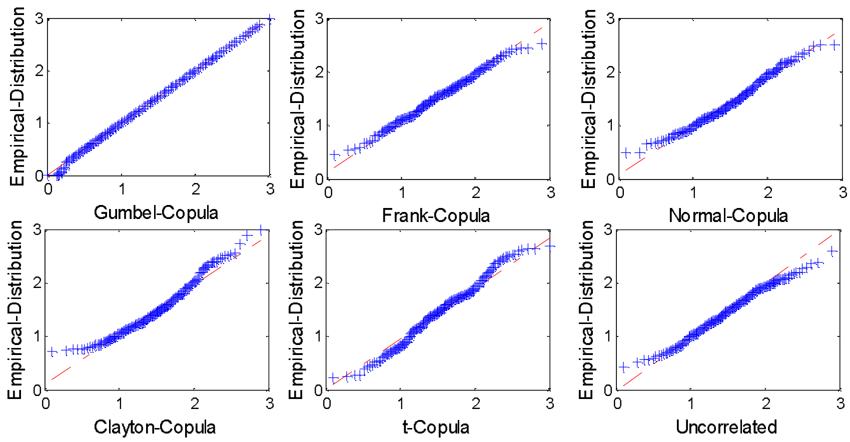

Figure 7: QQ plots for different Copula functions

Table 6: Optimal result comparison with global descent and primal-dual interior point algorithms

Bus	Global Descent Algorithm		Primal-dual Interior Point Algorithm	
	Electricity	Heat/Cold Energy	Electricity	Heat/Cold Energy
1	160.86	148.21	161.08	148.02
5	117.25	175.25	117.11	175.53
8	76.77	-	76.39	-
10	-	50.00	-	50.31
13	87.75	112.54	88.07	112.14
15	75.62	-	75.20	-
Cost ($)	6133.0		6143.7	
Calculation Time (s)	11.271		15.522	

8 and 15, the proposed optimization model formulated in this paper is then solved (the number of sampling in SAA is set as 5000), and the resulting system cost is 6133.0$. On the other hand, if the two wind power outputs are assumed to be independent, the corresponding system cost will be 6310.8$. Therefore, by modelling the correlation between multiple wind power outputs, the sys-tem cost can be decreased by 177.8$, or 2.9%, as shown in Table 7. The accuracy and economy of CCHP system can be improved.

2) The Impacts of Emission Trading

The optimal scheduling results with and without considering emissions trading are shown in Table 8. Suppose the price of emissions trading fluctuates in the range of 0$/ton-10$/ton (i.e. the expected mean varies between [0,10], and the variance is constant, set as 1.3), the impacts of price fluctuation on electrical/heat/cold energy generated by CCHP units as well as total system cost are shown in Figs. 8 and 9.

As can be seen in Table 8, the system cost is 5568$ without considering emission trading

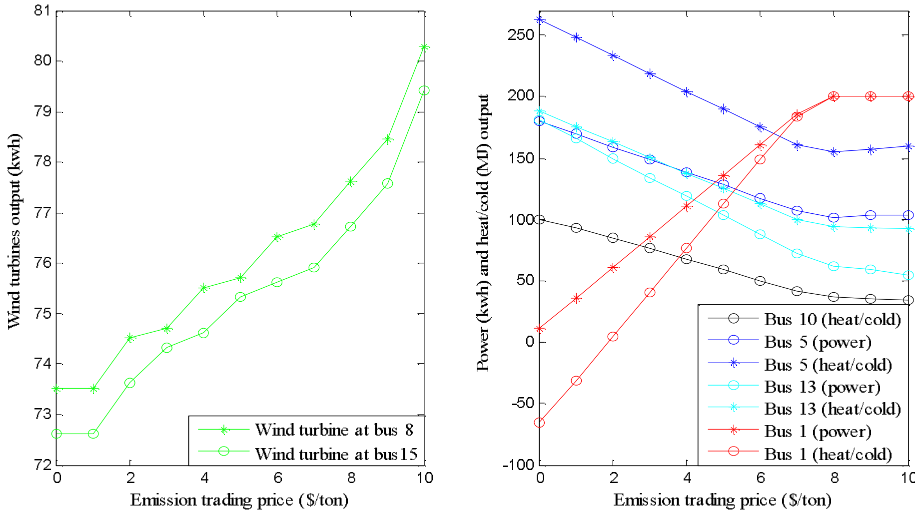

Figure 8: Scheduling results of CCHP units varying with the price of emissions trading

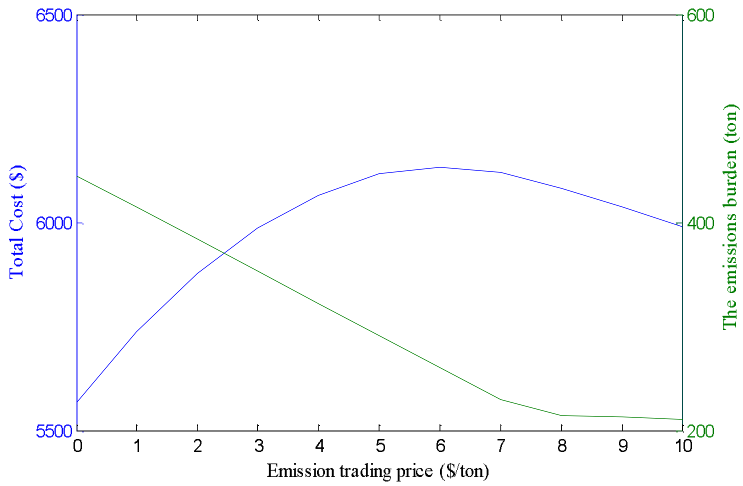

Figure 9: The total system cost and emissions burden varying with the price of emissions trading

Table 7: Optimal result comparison with global descent and primal-dual interior point algorithms

Bus	Independent Distribution		Joint Distribution	
	Electricity	Heat/Cold Energy	Electricity	Heat/Cold Energy
1	168.86	144.17	161.86	148.21
5	119.00	170.65	117.25	175.25
8	73.77	-	76.77	-
10	-	51.25	-	50.00
13	84.45	119.92	87.75	112.54
15	71.92	-	75.62	-
Cost ($)	6310.8		6133.0	

scheme. The total cost is lower than the situation when emission trading scheme is considered, but in this situation the outputs of fossil-fired units in the CCHP system are close to their rated capacity, and 65.09MJ of heat/cold energy been transmitted into the adjacent system through pipe network, which leads to serious pollution and cannot meet the requirement of environment protection.

Table 8: Optimal result comparison with global descent and primal-dual interior point algorithms

Bus	Without Emission Trading		With Emission Trading	
	Electricity	Heat/Cold Energy	Electricity	Heat/Cold Energy
1	10.86	-65.09	160.86	148.21
5	180.25	262.85	117.25	175.25
8	73.52	-	76.77	-
10	-	100	-	50.00
13	180.75	188.24	87.75	112.54
15	72.62	-	75.62	-
Cost ($)	5568.0		6133.0	

As shown in Figs. 8 and 9, when emission trading price is lower than 1$/ton, the fossil-fired units operate nearly at their rated capacity. When the price is higher than 1$/ton, the outputs of fossil-fired units are reduced, but the outputs of renewable units are increased correspondingly, and the total generated electrical/heat/cold energy can be reduced sharply. When the price is higher than 8$/ton, the CCHP system purchases energy from cleaner adjacent system. Therefore, under reasonable emissions trading price, the total system cost and emissions pollutant can be reduced, and the utilization of renewable energy are promoted.

3) The Impact of SAA Sampling Number

The scheduling results and their corresponding calculation time obtained by selecting different sampling number in the SAA (i.e. parameter M) are given in Table 9. As observed, with the increase of sampling number, the optimal scheduling results become more accurate. By taking the tradeoff between the result accuracy and calculation time, the sampling number in this study is set as 5000.

Table 9: Scheduling results for different sampling numbers

Sampling Number	Wind power output Bus 8	Wind power output Bus 15	Total Cost($)	Calculation Time (s)
1000	75.10	73.92	6153.5	5.143
2000	76.15	75.21	6138.4	7.984
5000	76.77	75.62	6133.0	11.435
10000	76.78	75.64	6134.0	18.324
20000	76.78	75.64	6133.1	35.761
50000	76.78	75.64	6133.1	62.837

6 Conclusions

In this paper, emission trading scheme is introduced to reduce GHGs emission, and then mathematical models of multi-network CCHP system is proposed. After that, the optimal scheduling model for multi-network CCHP system is presented. Based on the joint probability distribution of the available output of wind turbines, the objective function is developed, and the sampling aver-age approximation, function smoothing and global descent algorithm are employed to solve the optimization problem. Finally, one modified 15-bus system is used to verify the performance of the proposed model and optimization solver.

References

[1] N. Br, *An Introduction to Copulas*, Springer, New York, 2005, pp. 7–48.

[2] J.P.S. Catalao, H.M.I. Pousinho and V.M.F. Mendes, Optimal offering strategies for wind power producers considering uncertainty and risk, *IEEE Systems Journal* 6 (2012) 270–277.

[3] A.N. Celik, A statistical analysis of wind power density based on the Weibull and Rayleigh models at the southern region of Turkey, *Renewable Energy* 29 (2003) 593–604.

[4] Y. Chen, A.L. Liu and B.F. Hobbs, Economic and emissions implications of load-based, source-based, and first-seller emissions trading programs under California AB32, *Oper. Res.* 59 (2011) 696–712.

[5] "Combined heat and power - Effective energy solutions for a sustainable future". Oak Ridge National Laboratory, Sep. 2011.

[6] F. Fang, Q.H. Wang and Y. Shi, A novel optimal operational strategy for the CCHP system based on two oper-ating modes, *IEEE Transactions on Power Systems* 27 (2012) 1032–1041.

[7] M. Geidl and G. Andersson, Optimal power flow of multiple energy carriers, IEEE Transactions on Power Systems 22 (2007) 145–155.

[8] J. Hetzer, D.C. Yu and K. Bhattarai, An economic dispatch model incorporating wind power, *IEEE Transactions on Energy Conversion* 23 (2008) 603–611.

[9] M. Hofert, Sampling archimedean copulas, *Comput. Statist. Data Anal* 52 (2008) 5163–5174.

[10] T.D. Jin, Y. Tian, C.W. Zhang and D.W. Coit, Multicriteria planning for distributed wind generation under strategic maintenance, *IEEE Transactions on Power Delivery* 28 (2013) 357–367.

[11] P. Jirutitijaroen and C. Singh, Reliability constrained multi-area adequacy planning using stochastic program-ming with sample-average approximations, *IEEE Transactions on Power Systems* 23 (2008) 504–513.

[12] T. Krause, G. Andersson, K. Frohlich and A. Vaccaro, Multiple-energy carriers: Modeling of production, delivery, and consumption, *Proceedings of the IEEE.* 99 (2011) 15–27.

[13] X.H. Li and C.W. Jiang, Short-term operation model and risk management for wind power penetrated system in electricity market, *IEEE Transactions on Power Systems* 26 (2011) 932–939.

[14] P. Linares, F. Javier Santos, M. Ventosa and L. Lapiedra, Incorporating oligopoly, CO2 emissions trading and green certificates into a power generation expansion model, *Automatica* 44 (2008) 1608–1620.

[15] E. Mashhour and S.M. Moghaddas-Tafreshi, Bidding strategy of virtual power plant for participating in energy and spinning reserve markets-part II: numerical analysis, *IEEE Transactions on Power Systems* 26 (2011) 957–964.

[16] C.K. Ng, *High performance continuous/discrete global optimization methods*, Ph.D. Dissertation, Chinese University of Hong Kong, 2003.

[17] C.K. Ng, D. Li and L.S. Zhang, Global descent method for global optimization, *SIAM Journal on Optimization* 20 (2010) 3161–3184.

[18] X.J. Tong, L.Q. Qi, F. Wu and H. Zhou, A smoothing method for solving portfolio optimization with CVaR and applications in allocation of generation asset, *Appl. Math. Comput* 216 (2010) 1723–1740.

[19] M.T. Tsay, The operation strategy of cogeneration systems using a multi-objective approach, *IEEE Power Engineering Society Transmission and Distribution Conference* 3 (2002) 1653–1657.

[20] S. Villarreal, J.A. Jimenez, T.D. Jin and M. Cabrera-Rios, Designing a sustainable and distributed generation system for semiconductor wafer fabs, *IEEE Transactions on Automation Science and Engineering* 10 (2013) 16–26.

[21] Q.F. Wang, J.H. Wang and Y.P. Guan, Price-based unit commitment with wind power utilization constraints, *IEEE Transactions on Power Systems* 28 (2013) 1–9.

[22] L.N. Yu and E.O. Voit, Construction of bivariate s-distributions with copulas, *Comput. Statist. Data Anal.* 51 (2006) 1822–1839.

[23] Z. Yu, P.V. Preckel, G. Nderitu and F.T. Sparrow, A locational gaming model with CO2 emission tax and limits, *International Journal of Electrical Power & Energy Systems* 23 (2001) 451–457.

[24] J.H. Zhao, F.S. Wen, Z.Y. Dong, Y.S. Xue and K.P. Wong, Optimal dispatch of electric vehicles and wind power using enhanced particle swarm optimization, *IEEE Transactions on Industrial Informatics* 8 (2012) 889–899.

Manuscript received 29 March 2013
revised 27 August 2013
accepted for publication 13 October 2013

Hongming Yang
Hunan Province Key Laboratory of Smart Grids Operation and Control
School of Electrical Engineering and Information
Changsha Univercity of Science and Technology
Changsha, Hunan, 410114, China
E-mail address: yhm5218@hotmail.com

Dangqiang Zhang
Hunan Province Key Laboratory of Smart Grids Operation and Control
School of Electrical Engineering and Information
Changsha Univercity of Science and Technology
Changsha, Hunan, 410114, China
E-mail address: qqzdq@hotmail.com

Ke Meng
Centre for Intelligent Electricity Networks, The University of Newcastle
Callaghan, NSW 2308, Australia
E-mail address: ke.meng@newcastle.edu.au

Zhao Yang Dong
School of Electrical and Information Engineering
University of Sydney, Sydney, NSW 2006, Australia
E-mail address: joe.dong@sydney.edu.au

Mingyong Lai
Key Laboratory of Logistics Information and Simulation Technology
Hunan University, Changsha, Hunan, 410082, China
E-mail address: laimingyong0731@hotmail.com